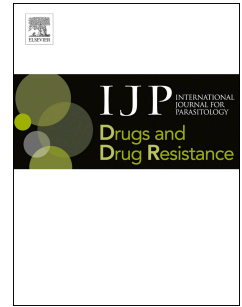


Accepted Manuscript

4-Nitro styrylquinoline is an antimalarial inhibiting multiple stages of *Plasmodium falciparum* asexual life cycle

Bracken F. Roberts, Yongsheng Zheng, Jacob Cleaveleand, Sukjun Lee, Eunyoung Lee, Lawrence Ayong, Yu Yuan, Debopam Chakrabarti



PII: S2211-3207(16)30138-5

DOI: [10.1016/j.ijpddr.2017.02.002](https://doi.org/10.1016/j.ijpddr.2017.02.002)

Reference: IJPDDR 175

To appear in: *International Journal for Parasitology: Drugs and Drug Resistance*

Received Date: 18 December 2016

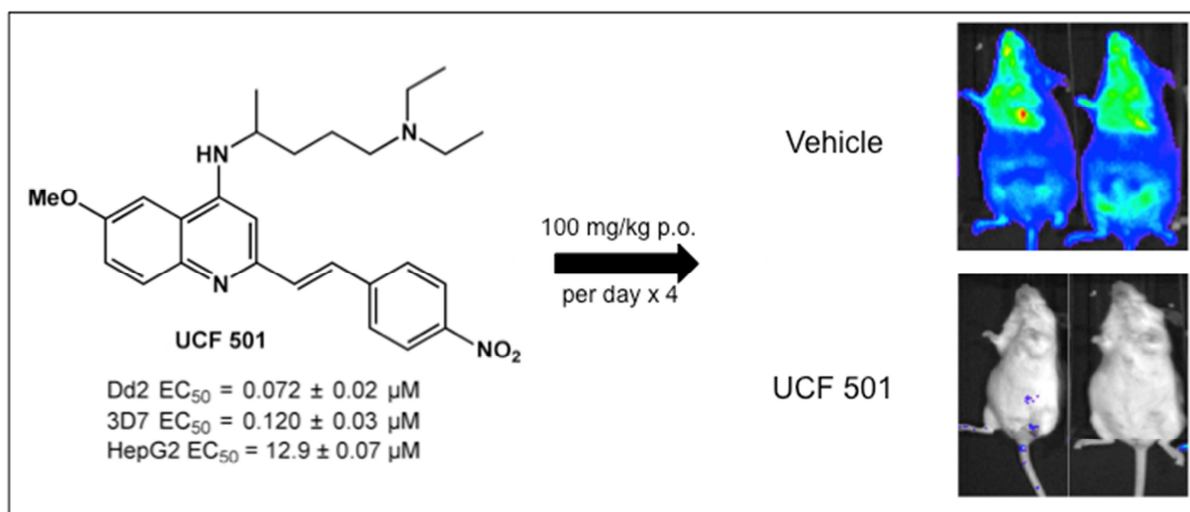
Revised Date: 13 February 2017

Accepted Date: 15 February 2017

Please cite this article as: Roberts, B.F., Zheng, Y., Cleaveleand, J., Lee, S., Lee, E., Ayong, L., Yuan, Y., Chakrabarti, D., 4-Nitro styrylquinoline is an antimalarial inhibiting multiple stages of *Plasmodium falciparum* asexual life cycle, *International Journal for Parasitology: Drugs and Drug Resistance* (2017), doi: 10.1016/j.ijpddr.2017.02.002.

This is a PDF file of an unedited manuscript that has been accepted for publication. As a service to our customers we are providing this early version of the manuscript. The manuscript will undergo copyediting, typesetting, and review of the resulting proof before it is published in its final form. Please note that during the production process errors may be discovered which could affect the content, and all legal disclaimers that apply to the journal pertain.

R1PT



AC

1 **4-Nitro Styrylquinoline is an Antimalarial Inhibiting Multiple**

2 **Stages of *Plasmodium falciparum* Asexual Life Cycle**

3

4

5 Bracken F. Roberts,^a Yongsheng Zheng,^b Jacob Cleaveleand,^b Sukjun

6 Lee^c, Eunyoung Lee^c, Lawrence Ayong,^d Yu Yuan,^b and Debopam

7 Chakrabarti^{a#}

8

9 Division of Molecular Microbiology, Burnett School of Biomedical Sciences, College
10 of Medicine, University of Central Florida, Orlando, Florida^a

11 Department of Chemistry, University of Central Florida, Orlando, Florida^b

12 Institut Pasteur Korea, Seongnam-si, Gyeonggi-do, Korea^c

13 Center Pasteur, Yaounde, Cameroon

14

15 Address correspondence to Debopam Chakrabarti, dchak@ucf.edu.

16

17 Running title: Styrylquinoline is a novel antimalarial compound

18 **Abstract**

19

20 Drugs against malaria are losing their effectiveness because of emerging drug
21 resistance. This underscores the need for novel therapeutic options for malaria with
22 mechanism of actions distinct from current antimalarials. To identify novel
23 pharmacophores against malaria we have screened compounds containing
24 structural features of natural products that are pharmacologically relevant. This
25 screening has identified a 4-nitro styrylquinoline (SQ) compound with submicromolar
26 antiplasmodial activity and excellent selectivity. SQ exhibits a cellular action distinct from
27 current antimalarials, acting early on malaria parasite's intraerythrocytic life cycle
28 including merozoite invasion. The compound is a fast-acting parasitocidal agent and also
29 exhibits curative property in the rodent malaria model when administered orally. In this
30 report, we describe the synthesis, preliminary structure-function analysis, and the
31 parasite developmental stage specific action of the SQ scaffold.

32

33

34

35

36

37 **Keywords:**

38

39 Antimalarials, antiplasmodials, natural-product-like compounds, styrylquinoline,
40 invasion inhibitor

41 1. Introduction

42 Malaria afflicts about half of the world's populations causing about 500,000 deaths
43 annually (World Health Organization., 2016). It is of great concern that the drugs
44 available for malaria therapy, including artemisinin, are rapidly becoming ineffective
45 because of the widespread prevalence of drug resistant parasites (Greenwood, 1995;
46 Rieckmann, 2006). Although artemisinin-based combination treatments (ACTs)
47 have been effective in controlling the disease in many malaria endemic areas, the
48 appearance of parasites resistant to artemisinin derivatives in wide areas of
49 Southeast Asia, from South Vietnam to central Myanmar, emphasizes the fragility
50 of available malaria treatment measures (Ashley et al., 2014; Cui, 2011).
51 Therefore, there is an urgent need for new drugs directed against novel cellular targets,
52 either for monotherapy or as a combination with other antimalarials that would result in
53 an immediate intervention in the asexual life cycle.

54 Natural product (NP)-derived compounds are the richest source of novel
55 pharmacophores as they are known to occupy biologically important chemical space
56 (Cordier et al., 2008; Genis et al., 2012; Rishton, 2008; Vasilevich et al., 2012). NPs also
57 have been pre-validated by nature, having gone through millions of years of natural
58 selection to develop their ability to interact with biological macromolecules (Bon and
59 Waldmann, 2010; Genis et al., 2012). Thus NPs exemplify unique structural elements
60 that can be exploited as pre-validated starting points for novel synthetic libraries (Bon and
61 Waldmann, 2010). Critical evaluations of known drugs and natural products have been
62 used to identify drug/NP-based substructural motifs, termed as "BioCores" (Kombarov et
63 al., 2010). To identify new antimalarial hits with novel mechanism of action, we have
64 screened a collection of compounds that incorporates features of "BioCore" and known
65 antimalarials. This screening effort has identified a 4-nitro styrylquinoline (SQ) as an

66 antiplasmodial pharmacophore. In this report, we present the initial structure activity
67 relationship based on this core structure, in vivo efficacy and stage specific activity.

68

69 **2. Materials and Methods**

70

71 *2.1. P. falciparum culture and Viability Assay.*

72 *P. falciparum* Dd2 (chloroquine-resistant) and 3D7 (chloroquine-sensitive) were
73 cultured in human A⁺ erythrocytes using a modified Trager and Jensen (Trager and
74 Jensen, 1976) method in RPMI 1640 medium with L-glutamine (Invitrogen) and
75 supplemented with 25 mM HEPES, pH 7.4, 26 mM NaHCO₃, 2% dextrose, 15 mg/L
76 hypoxanthine, 25 mg/L gentamycin, and 0.5% Albumax II. Cultures were maintained
77 at 37°C in 5% CO₂ and 95% air. Parasite viability was determined using a SYBR
78 green I-based assay (Bennett et al., 2004; Johnson et al., 2007; Smilkstein et al.,
79 2004). Different dilutions of the compound in DMSO were added to the *P. falciparum*
80 culture at a 1% parasitemia and 2% hematocrit in 96-well plates (SantaCruz
81 Biotechnology). Maximum DMSO concentration was less than 0.125%. Chloroquine
82 at 1 µM was used as a positive control to determine the baseline value. Following 72
83 h incubation at 37°C, the plates were frozen at -80°C. Plates were thawed and 100 µl
84 of lysis buffer (with 20 mM Tris-HCl, 0.08% saponin, 5 mM EDTA, 0.8% Triton X-
85 100, and 0.01% SYBR Green I) was added to each well. Fluorescence emission
86 from the plates was read using a Synergy H4 hybrid multimode plate reader (Biotek)
87 set at 485 nM excitation and 530 nM emission after incubation in the dark for 30
88 minutes at 37°C.

89

90 *2.2. Library of compounds for screening.*

91 To select unique chemotypes we divided 50,000 BioCore (BioDesign) compounds
92 (www.asinex.com) into clusters, using the cheminformatics software package Molsoft
93 ICM Chemist Pro (www.molsoft.com/icm_pro.html) and JKlustor (ChemAxon). This
94 analysis identified 2,115 clusters. A central compound from each cluster was
95 selected for purchase as this allowed us to maximize representation of the entire
96 library set at minimal cost.

97

98 2.3. Cytotoxicity Assay.

99 Compounds at different dilutions were assessed for cytotoxicity in 384 well clear
100 bottom plates (Santa Cruz Biotechnology) using HepG2 human hepatocyte cells at
101 2,500 cells/well. The plates were incubated for 48 h at 37° C in an atmosphere
102 containing 5% CO₂. Twenty µL MTS [(3-(4,5-dimethylthiazol-2-yl)-5-(3-
103 carboxymethoxyphenyl)-2-(4-sulfophenyl)-2H-tetrazolium), CellTiter 96® Aqueous
104 non-radioactive cell proliferation assay (Promega) reagent was added to each well
105 and the plates were incubated for an additional 3 h. Cell viability was obtained by
106 measuring the absorbance at 490 nm using Synergy H4 hybrid multimode plate
107 reader (BioTek).

108

109 2.4. Physicochemical Parameters.

110 The aqueous solubility at pH 7.4 was assessed by UV-visible absorption based
111 method (Avdeef, 2001). The permeability was evaluated by the *in vitro* double-sink
112 parallel artificial membrane permeability assay (Kansy et al., 1998) that is a model
113 for the passive transport from the gastrointestinal tract into the blood stream. The
114 microsomal stability (Janiszewski et al., 2001) was determined by incubating the
115 compound with mouse liver microsomes in the presence or absence of NADPH.

116

117 *2.5. General Chemistry.*

118 All chemicals and solvents were purchased from commercial vendors and used
119 without further purification unless otherwise noted. Analytical TLC was performed
120 with Silicycle silica gel 60 F254 plates; visualized by means of a UV light or spraying
121 with chemical stains. Chromatography was performed with Silicycle silica gel (230-
122 400 mesh) and using appropriate solvents as eluent. NMR spectra were recorded on
123 a Bruker AV-400 or a Varian VNMRs 500 spectrometer. Proton chemical shifts were
124 referenced relative to residual CDCl₃ proton signals at δ 7.27 ppm. Data for ¹H NMR
125 are reported as follows: chemical shift (ppm), multiplicity (s = singlet, d = doublet, t =
126 triplet, q = quartet, brs = broad singlet, m = multiplet), coupling constants (Hz),
127 integration. Mass spectra were recorded on an Agilent 6230 TOF LCMS instrument.
128 Compounds **2** and **3** were prepared according to the previous literature procedures
129 (Thomas et al., 2010). Additional general chemistry procedures are presented as
130 supplementary content.

131

132 *2.6. β -Hematin formation assay.*

133 Compounds were tested for inhibition of β -hematin formation using the method
134 described in Sandlin *et al* (Sandlin et al., 2011). Briefly, 100 μ M (final concentration)
135 of compound was added to 384 well flat bottom plates (SantaCruz Biotechnology)
136 followed by the addition of 20 μ L water, 7 μ L of acetone and 5 μ L of 348 μ M Nonidet
137 P-40. Twenty five μ L of 228 μ M hematin-DMSO suspension was added to each well
138 and the plate was incubated at 37° C in a shaking incubator for 6 hours. β -hematin
139 formation was analyzed using pyridine ferrochrome assay (Ncokazi and Egan,
140 2005). In essence, 5% v/v final concentration of pyridine from a solution consisting

141 of water, 20% acetone, 200 mM HEPES and 50% pyridine was used and incubated
142 under the same conditions as above for 10 minutes. Resulting pyridine-ferrochrome
143 complex was measured at 405 nm using Biotek Synergy H1 multireader.

144

145 2.7. Cellular Inhibition Mechanisms.

146 *P. falciparum* Dd2 cultures were synchronized by magnetic separation of schizonts
147 (Ribaut et al., 2008), followed by sorbitol treatment (Lambros and Vanderberg,
148 1979). Synchronized cultures were treated at 6, 18, 30, 42 h post-invasion with UCF
149 501 at 5 x EC₅₀, Giemsa-stained thin smears were prepared at 12 h time intervals,
150 and microscopically evaluated to assess the block in intraerythrocytic maturation.
151 Samples were also collected at these time intervals fixed in a solution containing
152 0.04% glutaraldehyde in PBS, permeabilized with 0.25% Triton X-100, treated with
153 RNase (50 µg/ml) and stained with 10.24 µM YOYO-1 (Bouillon et al., 2013). Flow
154 cytometry acquisition was performed in ThermoFisher Attune NxT at a voltage of 260
155 with excitation wavelength of 488 nM and an optical filter of 530/30.

156 The effect of UCF 501 on merozoite egress and invasion was also analyzed
157 by an image-based assay described previously (Roberts et al., 2016). Briefly,
158 synchronized *P. falciparum* HB3 (chloroquine-sensitive) at 1.5% hematocrit and 5%
159 parasitemia was exposed to each of N-acetylglucosamine (GlcNAc), E-64,
160 artemisinin and UCF 501 at 10 µM final concentration for 24 h. The culture was then
161 stained with wheat germ agglutinin-Alexa Fluor 488 conjugate and Mitotracker Red
162 CMXRos each at 1 nM final concentrations, and incubated at 37°C for 20 min. The
163 culture was next fixed in a solution containing 4% paraformaldehyde and 5 µg/ml
164 DAPI (4',6-diamidino-2-phenylindole). Five image fields were captured at three
165 wavelengths (405 nM, DAPI; 488 nM, Alexa fluor; and 635 nM, Mitotracker deep red)

166 using Operetta 2.0 automated imaging system (Perkin Elmer) from each assay well
167 (384-well glass plate, Matrical) with a 40X high numerical aperture objective.

168

169 2.8. *In vivo Efficacy Determination.*

170 Standard variations of the Peters' four-day test (Peters, 1975; Sanni et al., 2002) with the
171 compound following oral administration was used to test the *in vivo* efficacy in the murine
172 malaria model using the *P. berghei* ANKA strain (Neill and Hunt, 1992). Female
173 pathogen-free balb/c mice (8 weeks, ~25 g, 5 animals/group) were infected with 1×10^6
174 parasitized RBC (from a donor mouse) harboring *P. berghei* ANKA, by intraperitoneal
175 (i.p.) injection. The animals were administered with the test compound by oral gavage
176 (0.2 ml/dose), at 100mg/kg twice daily for 4 consecutive days starting 6hr post-infection.
177 Test compound UCF 501 was formulated in 0.5% hydroxyethylcellulose-0.1% Tween 80.
178 The control group had only the vehicle. Thin blood smears were made from blood droplet
179 from the temporal vein and Giemsa-stained for microscopic evaluation of parasitemia on
180 day 4 and every day thereafter for 10 days and every other day beyond that. Mice were
181 euthanized when parasitemia reached 40%. The animals were considered cured when
182 smears were negative 30 days post infection. Elimination of existing infection was tested
183 in Swiss Webster mice infected with 10^4 *P. berghei* ANKA expressing luciferase on day 0.
184 Seventy two hours post infection mice were grouped (n=5 per group) and received either
185 vehicle (200 μ L, 2% methylcellulose, 0.5% Tween80), chloroquine (200 μ L, 40 mg/kg), or
186 UCF 501 (200 μ L, 100 mg/kg), via oral gavage once daily for 5 days at the Anti-Infectives
187 Screening Core at New York Langone Medical Center, New York University (NYU). On
188 day 7 post-infection, the mice were injected with 150 mg/kg of D-luciferin potassium salt
189 substrate in PBS, and imaged in an *in vivo* imaging system (IVIS, Lumina II, Perkin

190 Elmer). The study was conducted using a protocol approved by the UCF and NYU
191 institutional animal care and use committees (IACUC).

192

193 **3. Results and discussion**

194

195 *3.1. Discovery of 4-nitro styrylquinoline (UCF 501) as selective antiplasmodial* 196 *compound*

197 To discover innovative antimalarial compounds that act on new cellular targets, we
198 screened a library of 2,115 compounds selected from the BioDesign and Biomimetic
199 (also known as BioCore) platforms of the chemical compound vendor Asinex, which
200 incorporates structural features of pharmacologically relevant natural products. We
201 used an unbiased cell-based screen utilizing SYBR green I-based assay (Bennett et
202 al., 2004; Johnson et al., 2007; Smilkstein et al., 2004) to identify antiplasmodial
203 activities. For our primary screen, we used the chloroquine-resistant Dd2 strain and
204 a stringent criterion of $IC_{50} < 500$ nM. We identified 39 unique scaffolds (1.8%) as initial
205 hits based on the criterion. A 4-nitro styrylquinoline (SQ, UCF 501), exhibiting excellent
206 antiplasmodial potency with an EC_{50} value of 67 nM (Table 1) was the most potent of
207 these compounds. Furthermore, this chemotype exhibited better EC_{50} values for the
208 chloroquine resistant Dd2 strain compared to the chloroquine sensitive 3D7 line,
209 indicating that the compound may function differently from chloroquine. The EC_{50} for
210 chloroquine is 15-fold higher in Dd2 (0.172 μ M) compared to the 3D7 (0.011 μ M)
211 line. As a counter screen, we evaluated the cytotoxicity of these compounds in
212 human hepatocyte cell line HepG2 using a MTS cell proliferation assay (Gupta et al.,
213 2009). The EC_{50} value of UCF 501 in HepG2 cells was 12.9 μ M demonstrating an
214 excellent selectivity of 192 (Table 1).

215

216 **3.2. Physicochemical properties and structure-activity relationship of UCF 501**

217 We evaluated the compliance of UCF 501 with Lipinski's parameters. We also
218 determined the *in vitro* physicochemical profiles (Avdeef, 2001) of UCF 501. As can be
219 seen from the data presented in Table 2, the compound is in compliance with the
220 Lipinski's parameters, and possesses good permeability and solubility. UCF 501 has a
221 microsomal stability ($t_{1/2}$) close to 1 h, which is considered an acceptable value. It has
222 been shown that compounds with similar microsomal stability are not expected to have
223 significant *in vivo* clearance liabilities based on pharmacokinetic studies using 306 real
224 world drug leads (Di et al., 2008).

225 The optimal physicochemical properties of UCF 501, in conjunction with its
226 mouse microsomal stability profiles, make the SQ compound series an attractive
227 platform for SAR studies. The preparation of arylvinylquinolines **8-17** and **20** are
228 illustrated in Fig. 1. The key intermediate chloroquinoline **3** was synthesized from
229 anisidine**1** and ethyl acetoacetate in 3 steps according to reported literature
230 procedures (Thomas et al., 2010). The replacement of chloride by various amino
231 groups was achieved by 2 different means. When an amino group is attached to the
232 flanking end of the alkyl chain, a direct nucleophilic aromatic addition-elimination
233 reaction ($S_{\text{N}}\text{Ar}$) is able to convert **3** to the corresponding aminoquinoline (**5** or **6**) at
234 elevated temperature (Gong et al., 2013); in contrast, when an amino group is
235 attached to a secondary position such as **19**, a palladium catalyzed amination
236 reaction proved to be more effective (Margolis et al., 2007). The addition of the styryl
237 group, the *trans*-selective olefination reaction of 2-methylquinoline was accomplished
238 by mixing desired aldehyde with quinoline in the presence of *p*-toluenesulfonamide
239 and the reaction proceeded through an enamine intermediate (Yan et al., 2011).

240 In the work presented here we attempted to address two important questions.
241 First of all, because the lead compound UCF 501 (**20**) has a chiral center (indicated
242 by an asterisk symbol in Fig 1) and its racemic form was used for the initial
243 screening, SAR study of different amino groups at the quinoline 4 position will
244 provide valuable information about the structural requirement for the antiplasmodial
245 activity. Second, the potential cytotoxicity issue associated with the nitro group on
246 the phenyl ring mandates a screening of the aromatic moiety in order to identify
247 proper surrogate groups for future development. For these reasons, we have
248 prepared SQs **8-17**, and their antiplasmodial activities are summarized in Table 3.
249 We first replaced the chiral amine moiety in UCF 501 with 3- morpholinopropylamine
250 and 3-dimethylaminopropylamine and compound **12** showed even better activity
251 profiles compared to UCF 501, which indicated that a chiral center on the amino
252 group alkyl chain was not necessary. The styryl group screening is focused on
253 substitution of the aromatic group. When phenyl, 4-fluorophenyl, 4-
254 trifluoromethylphenyl and 4-methoxycarbonylphenyl groups are incorporated into the
255 quinoline core structure, the resulting SQ analogues all possess submicromolar
256 activity against malaria parasites. Although nitro group analogues **12** and **17** are still
257 the most potent compounds in each series, the EC₅₀ values of 4-fluoro analogue **9**
258 and 4- methoxycarbonyl analogue **11** are close to that of UCF 501, which makes
259 them as good backup molecules if UCF 501 shows toxicity concerns in future
260 development. Nitroaromatic compounds such as UCF 501 may be flagged as 'structural
261 alert' because of potential toxicity issues (Walsh and Miwa, 2011). However,
262 nitroaromatic drugs are in use to treat a wide variety of diseases, including parasitic
263 diseases (Hemphill et al., 2006; Mattila and Larni, 1980; Pal et al., 2009; Raether and
264 Hanel, 2003; Sorkin et al., 1985; Truong, 2009; Wilkinson et al., 2011).

265

266 *3.3. UCF 501 does not inhibit β -hematin formation*

267 Given the quinoline-based chemical structure of SQ, we assessed the
268 inhibitory effect of UCF 501 on synthetic hemozoin (β -hematin) to rule out the
269 possibility of hemozoin formation inhibition as seen with quinoline antimalarials such
270 as, chloroquine and amodiaquine. We used a recently developed assay (Sandlin et
271 al., 2011), which uses Nonidet P-40, a lipophilic detergent, as a surrogate for lipid-
272 rich milieu of parasite's digestive vacuole. As evident from Table 4, while
273 chloroquine, a known inhibitor of β -hematin formation, exhibited complete inhibition
274 in this assay, UCF 501 is totally inactive. This result confirms that UCF 501, although
275 a 4-aminoquinoline compound unlike chloroquine does not target hemozoin
276 formation.

277

278 *3.4. Stage specificity of UCF 501 growth inhibition*

279 Next, we defined the developmental stage specific action of UCF 501 by both
280 microscopy and flow cytometry. Precise delineation of the timing of action of an
281 inhibitor provides valuable insight into the developmental growth and clinical
282 clearance of the parasite. Recent flow cytometry-based analysis of twelve antimalarials,
283 including ten that are widely used clinically, show that only artemisinin, artesunate,
284 cycloheximide, and trichostatin A have significant effect on parasite's ring stage (Wilson
285 et al., 2013). Furthermore, only artemisinin exhibited significant activity against schizonts,
286 and none of the antimalarials prevented the invasion of merozoites (Wilson et al., 2013).
287 Determination of stage-specificity also alludes to the mechanism of action of the UCF 501
288 and establishes if it is distinct from current antimalarials. To define the stage-
289 specificities antiplasmodial action of UCF 501, we investigated its effects on the

290 intraerythrocytic development of the parasite. Malaria parasite merozoites following
291 invasion of erythrocytes matures through a series of developmental stages termed
292 ring, trophozoite, schizont, and segmenter. Synchronized parasites were treated with
293 5 x EC₅₀ concentration at 6 (early ring), 18 (late ring/early trophozoite), 30 (early
294 schizont), 42 (mature schizont/segmenters) hours post invasion of erythrocytes by
295 merozoites and subsequently monitored at different post-invasion time-points (at 12
296 h intervals) for parasite cell cycle progression. As can be seen from Fig. 2, compared
297 to the untreated cultures UCF 501 rapidly inhibited parasite's development from the
298 early ring (Fig 2A), late ring/trophozoite (Fig 2B), and schizont stages (Fig 2C).
299 However, the compound was inactive in blocking merozoite egress as revealed by
300 absence of schizonts in the treated cultures (Fig 2D). When the culture was exposed
301 to UCF 501 at 42 hours post-invasion (hpi) ring-infected erythrocytes were scarcely
302 seen compared to the untreated controls (Fig 2D), suggesting a block in the invasion
303 of merozoites. These findings on development stage specific action of UCF 501 were
304 corroborated by flow cytometric analysis. The 6 hpi synchronized culture at the early
305 ring stage was treated at 5 x EC₅₀ concentration, followed by withdrawal of aliquots
306 at 12 h intervals to label the fixed parasite with YOYO-1 dye for flow cytometric
307 assessment. As seen in Fig. 3, at 6 hpi (early ring) in the control culture the peaks
308 represent singly, and multiple-infected cells based on DNA content. As the parasite
309 matures, the DNA content increases and peaks start to spread because of
310 schizogony. Following reinvasion parasitemia increases in the next growth cycle,
311 which is represented by an increase in peak heights. At 54 hpi parasites are at the
312 early ring stage of the next cycle, parasitemia is significantly higher, and three
313 distinct peaks reappear. In contrast, exposure to UCF 501 and artemisinin at the ring
314 stage (6 hpi) the maturation is blocked and as a result parasitemia does not

315 increase. This suggests a block of intraerythrocytic maturation of parasite early in the
316 developmental cycle when treated with UCF 501.

317 To further define the effects of UCF 501 on merozoite egress and invasion
318 processes, we analyzed developmental maturation of parasite following exposure to
319 UCF 501 using an image-based assay (Lee et al., 2014; Moon et al., 2013). As
320 shown in Fig. 4, when the synchronized culture was exposed to UCF 501 at 42 hpi at
321 the schizont stage, the DMSO (vehicle) treated culture showed rings inside RBC
322 after 24 h of growth. The artemisinin treated culture had similar effect as the drug
323 has no effect on invasion. E-64 (L-trans-epoxysuccinyl-leucylamido-(4-
324 guanidino)butane, a cysteine protease inhibitor, completely blocks egress as shown
325 by the presence of schizonts. In contrast, both N-acetylglucosamine (GlcNAc) and
326 UCF 501 blocks invasion as evidenced by the presence of extracellular merozoites
327 and absence of intracellular rings. N-acetylglucosamine is a reference invasion
328 inhibitor (Howard and Miller, 1981).

329 To confirm the effect of UCF 501 on merozoite invasion of new cells, we
330 quantified the parasitemia following treatment with the compound at the 42 h post-
331 invasion time point for 24 h. As can be seen from Fig. 5, there is a significant
332 reduction in culture parasitemia upon exposure to UCF 501 at 42 hpi compared to
333 control cultures. In contrast artemisinin, which has no influence on merozoite
334 invasion, does not cause similar marked reduction. These data suggest that UCF
335 501 has a significant effect on the merozoite viability and/or host cell invasion
336 process. Collectively, the above data suggest that the molecular targets of the
337 compound are likely to be essential for the merozoite survival and invasion
338 processes, and for the early ring to the mid-trophozoite developmental stage. Further
339 mechanistic characterization of the stage specific effect of UCF 501 will be the focus

340 of future studies. These results underscore the novelty of the mechanism of action
341 UCF 501 as it is distinct from current antimalarials which target either (a) the food
342 vacuole of late-ring and trophozoite stage parasites, (b) the biosynthesis of folic acid in
343 trophozoites (c) mitochondrion electron transport or (d) apicoplast translation (Dahl and
344 Rosenthal, 2007; Famin and Ginsburg, 2002; Goodman et al., 2007; Krishna et al., 2004;
345 Loria et al., 1999; Srivastava et al., 1997; Wilson et al., 2013).

346

347 *3.5. UCF 501 is a fast-acting parasitocidal compound*

348 Next, we assessed parasitocidal or parasitostatic properties of UCF 501, and if it
349 is parasitocidal, then what would be the optimum time to achieve the 100% parasitocidal
350 effect. Growing asynchronous parasites were exposed to 3 x EC₅₀ concentration of UCF
351 501 (200 nM) and artemisinin (45 nM) for 6, 12, 24 and 48 h followed by washing to
352 remove the inhibitor and continue monitoring growth for 144 h. Parasitemia decreased
353 significantly for both UCF 501 and artemisinin following 6 h exposure, although UCF 501
354 was more effective. Viable parasites showed signs of growth after 96 h following removal
355 of drug (Fig. 6A). However, 12 h (Fig. 6B) or longer exposure (not shown) to UCF 501
356 resulted in complete loss of viability. In contrast, we observed that a total loss of viability
357 could only be achieved with artemisinin at 3 x EC₅₀ concentration after 72 h of drug
358 exposure (data not shown). Similar time course of artemisinin action has been reported
359 earlier (Alin and Bjorkman, 1994). Furthermore, there was no sign of parasite recovery
360 observed for up to one week. The results described above establishes that UCF 501 is a
361 fast-acting parasitocidal agent.

362

363 *3.6. UCF 501 cures malaria in the rodent model*

364 Because of excellent *in vitro* activity and novel stage-specific action of UCF
365 501, we evaluated the potential of this scaffold to cure malaria using the rodent
366 malaria model. We used the *P. berghei* ANKA strain for infecting Balb/c mice as this
367 strain produces histopathological and immunopathological features that are strikingly
368 similar to human cerebral malaria (Neill and Hunt, 1992). As can be seen from Fig.
369 7A, UCF 501 cured malaria infection in mice when exposed to 100 mg/kg twice daily
370 by oral administration in 4/5 mice in a standard Peters' four-day test (Peters, 1975;
371 Sanni et al., 2002) when infection was initiated with 1×10^6 *P. berghei* ANKA cells, and the
372 treatment was initiated 4 h post-infection. All four surviving mice did not show any
373 evidence of infection up to day 30 and the parasitemia in one animal was 0.2% on
374 day 22 and reached 40% on day 27, when it was euthanized. To assess the ability of
375 UCF 501 to eliminate an established infection, treatment of animals was initiated 72h
376 post-infection. As can be seen from Fig 7B, the delayed treatment almost cleared
377 luciferase expressing parasite burden at 100 mg/kg once daily dose. Cure of malaria
378 in the rodent model by UCF 501 is very significant because the *P. berghei* model is
379 quite challenging, as it requires complete elimination of parasites, otherwise fatal
380 parasitemia would recrudescence (Nallan et al., 2005). It is expected that with future
381 optimization of SQ scaffold much improved *in vivo* efficacy could be achieved.

382

383 4. Conclusion

384

385 In spite of widespread resistance to 4-aminoquinolines (4-AQ) compounds,
386 quinoline scaffold is still considered useful for the development of new generation of
387 antimalarials and many attractive 4-AQ analogs have been synthesized recently
388 (Saenz et al., 2012; Singh, 2009; Sinha et al., 2014; Tukulula et al., 2013). Although

389 these newer generation of AQ analogs do not exhibit cross-resistance to
390 chloroquine, it is unknown if their mechanisms of action are distinct from that of
391 chloroquine. Many of these new AQ analogs are either known to inhibit β -hematin
392 formation with IC_{50} in the submicromolar range, or their interaction with β -hematin is
393 as yet unpublished. In that respect the absence of β -hematin inhibitory activity of
394 UCF 501 is noteworthy. Furthermore, UCF 501, acts quickly (phenotypically observable
395 developmental changes within 12 hours of treatment) at all stages of the intraerythrocytic
396 lifecycle. It is significant that UCF 501 inhibits merozoite invasion unlike any other
397 approved drugs for malaria. This novel cellular action provides strong evidence that the
398 SQ chemotype potentially is a new therapeutic option for malaria directed against unique
399 cellular targets. Future isobologram analysis with lead compounds will define the utility of
400 the SQ chemotype in combination therapies. In summary, our results suggest that SQ
401 analogs in its ability to block all stages of parasite intraerythrocytic development, and
402 rapidly clear parasites have immense potential as an antimalarial pharmacophore.

403

404 **ACKNOWLEDGEMENTS**

405 This work was supported by Burnett School of Biomedical Sciences Director's
406 Impact Award, UCF College of Medicine research development intramural award,
407 and NIH/NIAID AI117298. We thank Robert Banks at the UCF Animal Care Facility
408 for his assistance and training with the BALB/c mice experiments. We also thank
409 Ana Rodriguez at NYULMC for the IVIS imaging experiment.

410

411 **ABBREVIATION USED**

412 BINAP, 2,2'-bis(diphenylphosphino)-1,1'-binaphthyl; *p*-TsNH₂, *p*-toluenesulfonamide.

413

414 **REFERENCES**

- 415 Alin, M.H., Bjorkman, A., 1994. Concentration and time dependency of artemisinin
416 efficacy against *Plasmodium falciparum* in vitro. *The American journal of tropical*
417 *medicine and hygiene* 50, 771-776.
- 418 Ashley, E.A., Dhorda, M., Fairhurst, R.M., Amaratunga, C., Lim, P., Suon, S., Sreng,
419 S., Anderson, J.M., Mao, S., Sam, B., Sopha, C., Chuor, C.M., Nguon, C.,
420 Sovannaroeth, S., Pukrittayakamee, S., Jittamala, P., Chotivanich, K., Chutasmit, K.,
421 Suchatsoonthorn, C., Runchaoren, R., Hien, T.T., Thuy-Nhien, N.T., Thanh, N.V.,
422 Phu, N.H., Htut, Y., Han, K.T., Aye, K.H., Mokuolu, O.A., Olaosebikan, R.R.,
423 Folaranmi, O.O., Mayxay, M., Khanthavong, M., Hongvanthong, B., Newton, P.N.,
424 Onyamboko, M.A., Fanello, C.I., Tshefu, A.K., Mishra, N., Valecha, N., Phyo, A.P.,
425 Nosten, F., Yi, P., Tripura, R., Borrmann, S., Bashraheil, M., Peshu, J., Faiz, M.A.,
426 Ghose, A., Hossain, M.A., Samad, R., Rahman, M.R., Hasan, M.M., Islam, A.,
427 Miotto, O., Amato, R., MacInnis, B., Stalker, J., Kwiatkowski, D.P., Bozdech, Z.,
428 Jeeyapant, A., Cheah, P.Y., Sakulthaew, T., Chalk, J., Intharabut, B., Silamut, K.,
429 Lee, S.J., Vihokhern, B., Kunasol, C., Imwong, M., Tarning, J., Taylor, W.J., Yeung,
430 S., Woodrow, C.J., Flegg, J.A., Das, D., Smith, J., Venkatesan, M., Plowe, C.V.,
431 Stepniewska, K., Guerin, P.J., Dondorp, A.M., Day, N.P., White, N.J., Tracking
432 Resistance to Artemisinin, C., 2014. Spread of artemisinin resistance in *Plasmodium*
433 *falciparum* malaria. *The New England journal of medicine* 371, 411-423.
- 434 Avdeef, A., 2001. Physicochemical profiling (solubility, permeability and charge
435 state). *Current topics in medicinal chemistry* 1, 277-351.
- 436 Bennett, T.N., Paguio, M., Gligorijevic, B., Seudieu, C., Kosar, A.D., Davidson, E.,
437 Roepe, P.D., 2004. Novel, rapid, and inexpensive cell-based quantification of
438 antimalarial drug efficacy. *Antimicrob. Agents Chemother.* 48, 1807-1810.

- 439 Bon, R.S., Waldmann, H., 2010. Bioactivity-guided navigation of chemical space.
440 Accounts of chemical research 43, 1103-1114.
- 441 Bouillon, A., Gorgette, O., Mercereau-Puijalon, O., Barale, J.C., 2013. Screening and
442 evaluation of inhibitors of Plasmodium falciparum merozoite egress and invasion
443 using cytometry. Methods in molecular biology 923, 523-534.
- 444 Cordier, C., Morton, D., Murrison, S., Nelson, A., O'Leary-Steele, C., 2008. Natural
445 products as an inspiration in the diversity-oriented synthesis of bioactive compound
446 libraries. Natural product reports 25, 719-737.
- 447 Cui, W., 2011. WHO urges the phasing out of artemisinin based monotherapy for
448 malaria to reduce resistance. Bmj 342, d2793.
- 449 Dahl, E.L., Rosenthal, P.J., 2007. Multiple antibiotics exert delayed effects against
450 the Plasmodium falciparum apicoplast. Antimicrob. Agents Chemother. 51, 3485-
451 3490.
- 452 Di, L., Kerns, E.H., Ma, X.J., Huang, Y., Carter, G.T., 2008. Applications of high
453 throughput microsomal stability assay in drug discovery. Combinatorial chemistry &
454 high throughput screening 11, 469-476.
- 455 Famin, O., Ginsburg, H., 2002. Differential effects of 4-aminoquinoline-containing
456 antimalarial drugs on hemoglobin digestion in Plasmodium falciparum-infected
457 erythrocytes. Biochemical pharmacology 63, 393-398.
- 458 Genis, D., Kirpichenok, M., Kombarov, R., 2012. A minimalist fragment approach for
459 the design of natural-product-like synthetic scaffolds. Drug discovery today 17, 1170-
460 1174.
- 461 Gong, P., Zhai, X., Liu, Y., Zhao, Y., Zhang, F., Jiang, N., 2013. Preparation of 4-
462 aminoquinazoline derivatives as antitumor agents, Faming Zhuanli Shenqing.

- 463 Goodman, C.D., Su, V., McFadden, G.I., 2007. The effects of anti-bacterials on the
464 malaria parasite *Plasmodium falciparum*. *Molecular and biochemical parasitology*
465 152, 181-191.
- 466 Greenwood, D., 1995. Conflicts of interest: the genesis of synthetic antimalarial
467 agents in peace and war. *J Antimicrob Chemother* 36, 857-872.
- 468 Gupta, P.B., Onder, T.T., Jiang, G., Tao, K., Kuperwasser, C., Weinberg, R.A.,
469 Lander, E.S., 2009. Identification of selective inhibitors of cancer stem cells by high-
470 throughput screening. *Cell* 138, 645-659.
- 471 Hemphill, A., Mueller, J., Esposito, M., 2006. Nitazoxanide, a broad-spectrum
472 thiazolide anti-infective agent for the treatment of gastrointestinal infections. *Expert*
473 *opinion on pharmacotherapy* 7, 953-964.
- 474 Howard, R.J., Miller, L.H., 1981. Invasion of erythrocytes by malaria merozoites:
475 evidence for specific receptors involved in attachment and entry. *Ciba Foundation*
476 *symposium* 80, 202-219.
- 477 Janiszewski, J.S., Rogers, K.J., Whalen, K.M., Cole, M.J., Liston, T.E., Duchoslav,
478 E., Fouda, H.G., 2001. A high-capacity LC/MS system for the bioanalysis of samples
479 generated from plate-based metabolic screening. *Analytical chemistry* 73, 1495-
480 1501.
- 481 Johnson, J.D., Denuff, R.A., Gerena, L., Lopez-Sanchez, M., Roncal, N.E., Waters,
482 N.C., 2007. Assessment and continued validation of the malaria SYBR green I-
483 based fluorescence assay for use in malaria drug screening. *Antimicrob. Agents*
484 *Chemother.* 51, 1926-1933.
- 485 Kansy, M., Senner, F., Gubernator, K., 1998. Physicochemical high throughput
486 screening: parallel artificial membrane permeation assay in the description of
487 passive absorption processes. *Journal of medicinal chemistry* 41, 1007-1010.

- 488 Kombarov, R., Altieri, A., Genis, D., Kirpichenok, M., Kochubey, V., Rakitina, N.,
489 Titarenko, Z., 2010. BioCores: identification of a drug/natural product-based
490 privileged structural motif for small-molecule lead discovery. *Molecular diversity* 14,
491 193-200.
- 492 Krishna, S., Uhlemann, A.C., Haynes, R.K., 2004. Artemisinins: mechanisms of
493 action and potential for resistance. *Drug resistance updates : reviews and*
494 *commentaries in antimicrobial and anticancer chemotherapy* 7, 233-244.
- 495 Lambros, C., Vanderberg, J.P., 1979. Synchronization of *Plasmodium falciparum*
496 erythrocytic stages in culture. *The Journal of parasitology* 65, 418-420.
- 497 Lee, S., Lim, D., Lee, E., Lee, N., Lee, H.G., Cechetto, J., Liuzzi, M., Freitas-Junior,
498 L.H., Song, J.S., Bae, M.A., Oh, S., Ayong, L., Park, S.B., 2014. Discovery of
499 carbohybrid-based 2-aminopyrimidine analogues as a new class of rapid-acting
500 antimalarial agents using image-based cytological profiling assay. *J Med Chem* 57,
501 7425-7434.
- 502 Loria, P., Miller, S., Foley, M., Tilley, L., 1999. Inhibition of the peroxidative
503 degradation of haem as the basis of action of chloroquine and other quinoline
504 antimalarials. *The Biochemical journal* 339, 363-370.
- 505 Margolis, B.J., Long, K.A., Laird, D.L.T., Ruble, J.C., Pulley, S.R., 2007. Assembly of
506 4-aminoquinolines via palladium catalysis: A mild and convenient alternative to SNAr
507 methodology. *J. Org. Chem.* 72, 2232-2235.
- 508 Mattila, M.A., Larni, H.M., 1980. Flunitrazepam: a review of its pharmacological
509 properties and therapeutic use. *Drugs* 20, 353-374.
- 510 Moon, S., Lee, S., Kim, H., Freitas-Junior, L.H., Kang, M., Ayong, L., Hansen, M.A.,
511 2013. An image analysis algorithm for malaria parasite stage classification and
512 viability quantification. *PloS one* 8, e61812.

513 Nallan, L., Bauer, K.D., Bendale, P., Rivas, K., Yokoyama, K., Horney, C.P.,
514 Pendyala, P.R., Floyd, D., Lombardo, L.J., Williams, D.K., Hamilton, A., Sebti, S.,
515 Windsor, W.T., Weber, P.C., Buckner, F.S., Chakrabarti, D., Gelb, M.H., Van
516 Voorhis, W.C., 2005. Protein farnesyltransferase inhibitors exhibit potent antimalarial
517 activity. *Journal of medicinal chemistry* 48, 3704-3713.

518 Ncokazi, K.K., Egan, T.J., 2005. A colorimetric high-throughput beta-hematin
519 inhibition screening assay for use in the search for antimalarial compounds. *Anal.*
520 *Biochem.* 338, 306-319.

521 Neill, A.L., Hunt, N.H., 1992. Pathology of fatal and resolving *Plasmodium berghei*
522 cerebral malaria in mice. *Parasitology* 105 (Pt 2), 165-175.

523 Pal, D., Banerjee, S., Cui, J., Schwartz, A., Ghosh, S.K., Samuelson, J., 2009.
524 *Giardia*, *Entamoeba*, and *Trichomonas* enzymes activate metronidazole
525 (nitroreductases) and inactivate metronidazole (nitroimidazole reductases).
526 *Antimicrob. Agents Chemother.* 53, 458-464.

527 Peters, W., 1975. The chemotherapy of rodent malaria, XXII. The value of drug-
528 resistant strains of *P. berghei* in screening for blood schizontocidal activity. *Annals of*
529 *tropical medicine and parasitology* 69, 155-171.

530 Raether, W., Hanel, H., 2003. Nitroheterocyclic drugs with broad spectrum activity.
531 *Parasitology research* 90 Supp 1, S19-39.

532 Ribaut, C., Berry, A., Chevalley, S., Reybier, K., Morlais, I., Parzy, D., Nepveu, F.,
533 Benoit-Vical, F., Valentin, A., 2008. Concentration and purification by magnetic
534 separation of the erythrocytic stages of all human *Plasmodium* species. *Malaria*
535 *journal* 7, 45.

536 Rieckmann, K.H., 2006. The chequered history of malaria control: are new and
537 better tools the ultimate answer? *Ann Trop Med Parasitol* 100, 647-662.

- 538 Rishton, G.M., 2008. Molecular diversity in the context of leadlikeness: compound
539 properties that enable effective biochemical screening. *Current opinion in chemical*
540 *biology* 12, 340-351.
- 541 Roberts, B.F., Iyamu, I.D., Lee, S., Lee, E., Ayong, L., Kyle, D.E., Yuan, Y.,
542 Manetsch, R., Chakrabarti, D., 2016. Spirocyclic chromanes exhibit antiplasmodial
543 activities and inhibit all intraerythrocytic life cycle stages. *Int J Parasitol Drugs Drug*
544 *Resist* 6, 85-92.
- 545 Saenz, F.E., Mutka, T., Udenze, K., Oduola, A.M., Kyle, D.E., 2012. Novel 4-
546 aminoquinoline analogs highly active against the blood and sexual stages of
547 *Plasmodium* in vivo and in vitro. *Antimicrob. Agents Chemother.* 56, 4685-4692.
- 548 Sandlin, R.D., Carter, M.D., Lee, P.J., Auschwitz, J.M., Leed, S.E., Johnson, J.D.,
549 Wright, D.W., 2011. Use of the NP-40 detergent-mediated assay in discovery of
550 inhibitors of beta-hematin crystallization. *Antimicrob. Agents Chemother.* 55, 3363-
551 3369.
- 552 Sanni, L.A., Fonseca, L.F., Langhorne, J., 2002. Mouse models for erythrocytic-
553 stage malaria. *Methods in molecular medicine* 72, 57-76.
- 554 Singh, N.G., R.; Giulianotti, M.; Pinilla, C.; Houghten, R.; Medina-Franco, J. L., 2009.
555 Chemoinformatic Analysis of Drugs, Natural Products, Molecular Libraries Small
556 Molecule Repository and Combinatorial Libraries. *J. Chem. Inf. Model.* 49, 1010-
557 1024.
- 558 Sinha, M., Dola, V.R., Agarwal, P., Srivastava, K., Haq, W., Puri, S.K., Katti, S.B.,
559 2014. Antiplasmodial activity of new 4-aminoquinoline derivatives against
560 chloroquine resistant strain. *Bioorganic & medicinal chemistry* 22, 3573-3586.

- 561 Smilkstein, M., Sriwilaijaroen, N., Kelly, J.X., Wilairat, P., Riscoe, M., 2004. Simple
562 and inexpensive fluorescence-based technique for high-throughput antimalarial drug
563 screening. *Antimicrob. Agents Chemother.* 48, 1803-1806.
- 564 Sorkin, E.M., Clissold, S.P., Brogden, R.N., 1985. Nifedipine. A review of its
565 pharmacodynamic and pharmacokinetic properties, and therapeutic efficacy, in
566 ischaemic heart disease, hypertension and related cardiovascular disorders. *Drugs*
567 30, 182-274.
- 568 Srivastava, I.K., Rottenberg, H., Vaidya, A.B., 1997. Atovaquone, a broad spectrum
569 antiparasitic drug, collapses mitochondrial membrane potential in a malarial parasite.
570 *The Journal of biological chemistry* 272, 3961-3966.
- 571 Thomas, K.D., Adhikari, A.V., Shetty, N.S., 2010. Design, synthesis and
572 antimicrobial activities of some new quinoline derivatives carrying 1,2,3-triazole
573 moiety. *Eur. J. Med. Chem.* 45, 3803-3810.
- 574 Trager, W., Jensen, J.B., 1976. Human malaria parasites in continuous culture.
575 *Science* 193, 673-675.
- 576 Truong, D.D., 2009. Tolcapone: review of its pharmacology and use as adjunctive
577 therapy in patients with Parkinson's disease. *Clinical interventions in aging* 4, 109-
578 113.
- 579 Tukulula, M., Njoroge, M., Abay, E.T., Mugumbate, G.C., Wiesner, L., Taylor, D.,
580 Gibhard, L., Norman, J., Swart, K.J., Gut, J., Rosenthal, P.J., Barteau, S.,
581 Streckfuss, J., Kameni-Tcheudji, J., Chibale, K., 2013. Synthesis and in vitro and in
582 vivo pharmacological evaluation of new 4-aminoquinoline-based compounds. *ACS*
583 *medicinal chemistry letters* 4, 1198-1202.

584 Vasilevich, N.I., Kombarov, R.V., Genis, D.V., Kirpichenok, M.A., 2012. Lessons
585 from natural products chemistry can offer novel approaches for synthetic chemistry
586 in drug discovery. *Journal of medicinal chemistry* 55, 7003-7009.

587 Walsh, J.S., Miwa, G.T., 2011. Bioactivation of drugs: risk and drug design. *Annual*
588 *review of pharmacology and toxicology* 51, 145-167.

589 Wilkinson, S.R., Bot, C., Kelly, J.M., Hall, B.S., 2011. Trypanocidal activity of
590 nitroaromatic prodrugs: current treatments and future perspectives. *Current topics in*
591 *medicinal chemistry* 11, 2072-2084.

592 Wilson, D.W., Langer, C., Goodman, C.D., McFadden, G.I., Beeson, J.G., 2013.
593 Defining the timing of action of antimalarial drugs against *Plasmodium falciparum*.
594 *Antimicrob. Agents Chemother.* 57, 1455-1467.

595 World Health Organization., 2016. World malaria report 2016. World Health
596 Organization, Geneva, Switzerland.

597 Yan, Y., Xu, K., Fang, Y., Wang, Z., 2011. A Catalyst-Free Benzylic C-H Bond
598 Olefination of Azaarenes for Direct Mannich-like Reactions. *J. Org. Chem.* 76, 6849-
599 6855.

600

601

602 **Figure Legends**

603

604 **Fig. 1. Synthesis of compounds 1 to 20.** (a) ethyl acetoacetate, MgSO₄, HOAc,
605 EtOH, 90 °C; (b) Dowtherm, 270 °C; (c) POCl₃, reflux; (d) neat, pressure tube, 140
606 °C; (e) *m*-Xylene, *p*-TsNH₂, 140 °C; (f) Pd(OAc)₂, BINAP, K₃PO₄, 1,4-dioxane, 85 °C.
607 * symbol indicates chiral center.

608

609 **Fig. 2. UCF 501 blocks at multiple stages of intraerythrocytic development of**
610 ***P. falciparum*.** Tightly synchronized parasites were treated at (A) 6 h, (B) 18 h, (C)
611 30 h, and (D) 42 h post-invasion of merozoites with 5 x EC₅₀ concentration of the
612 compound. Microscopic evaluation of Giemsa-stained-thin smears were done at 12 h
613 intervals. Control represented infected red blood cells exposed to vehicle DMSO
614 (0.1%). hpi, hours post invasion of red blood cells by merozoites. Representative
615 figures from >80% of the infected RBCs are shown. Total number of observed
616 RBCs, overall parasitemia (P) and the respective number of rings (R), Trophozoites
617 (T), and Schizonts (S) are listed for each time point.

618

619

620 **Fig. 3. UCF 501 Inhibits *Plasmodium falciparum* early in the intraerythrocytic**
621 **cell cycle.** Tightly synchronized cultures were treated with UCF 501,
622 dihydroartemisinin (DHA), or vehicle at early ring stage (6 h post invasion) and then
623 monitored every 12 hours for a 48 hour period. YOYO-1 treated samples were read
624 on Attune NXT flow cytometer at a voltage of 260 with excitation wavelength of
625 488nm and an optical filter of 530/30. Side scatter (SSC) log/Forward scatter (FSC)
626 log density plots (A, top) and FSC log/YOYO-1 scatter plots (A, bottom) show distinct

627 RBC and iRBC populations. (B) UCF 501 was added to tightly synchronized parasite
628 cultures at A) 6 hours, B) 18 hours, C) 30 hours, and D) 42 hours post invasion and
629 then incubated for at least 24 hours. At 12-hour increments treated cultures were
630 fixed, permeabilized and stained with YOYO-1 for flow cytometry along with blood
631 smears for Giemsa staining. Plots represent cell count in y-axis versus FL1 channel
632 (488 nm Laser with 533/30 filter) representing DNA content. iRBC, infected red blood
633 cells.

634

635 **Fig. 4. Confocal plate micrograph showing parasite phenotype following 24h**
636 **compound exposure at 42 hpi (schizont stage).** Sorbitol-synchronized cultures
637 were treated at 1 μ M concentration of UCF 501 or the reference compounds E-64
638 (protease inhibitor blocking egress), GlcNAc (N-acetylglucosamine, invasion
639 inhibitor), or artemisinin at 42 hpi for 24 h. Cultures were then stained in a solution
640 containing 1 nM each of wheat germ agglutinin-Alexa Fluor 488 conjugate and
641 Mitotracker Red CMXRos followed by treatment with 4% paraformaldehyde and 5
642 μ g/ml DAPI (2-(4-Amidinophenyl)-6-indolecarbamide dihydrochloride, 4',6-
643 Diamidino-2-phenylindole dihydrochloride). Fluorescence imaging and automated
644 detection of parasitized erythrocytes was done in an Operetta 2.0 system. Sample
645 micrographs showing accumulation of extracellular merozoites in UCF 501 or
646 GlcNAc-treated cultures compared to late rings ("Ring") in the solvent control wells,
647 or schizonts in the E-64 and artemisinin-treated wells. The mitotracker-positive
648 infected erythrocytes are indicated as "Live" whereas mitotracker-negative cells are
649 labeled as "Dead".

650

651 **Fig. 5. Effect of UCF 501 on parasitemia when treated at the late**
652 **schizont/segmenter stage.** Cultures at 42 h post-invasion was exposed to UCF
653 501 or artemisinin at 5 x EC₅₀.

654

655 **Fig. 6. UCF 501 is parasitocidal.** Asynchronous cultures were exposed to 3 x EC₅₀
656 of UCF 501 (200 nM) or artemisinin (45 nM) for (A) 6 h, and (B) 12 h followed by
657 washing and growing in the absence of the inhibitors.

658

659 **Fig. 7. UCF 501 exhibits curative property.** (A) Effect of UCF 501 on the
660 survivability of *P. berghei* ANKA infected Balb/c mice was evaluated. Mice were
661 treated orally with UCF 501 twice daily at 100 mg/kg at the time of infection. (B & C)
662 Swiss Webster mice were infected with *P. berghei* ANKA expressing luciferase,
663 treated with 100 mg/kg orally once daily 72 hours post-infection, and the luciferin
664 signal was detected (B) and quantified (C) with an *in vivo* imaging system (IVIS).

Table 1. Activities of antiplasmodial scaffold UCF 501

EC₅₀ values (±SD) are derived from 3 independent experiments, each with 3 replicates. The Z' factors of these assays were >0.8. *P. falciparum* Dd2, chloroquine resistant; 3D7, chloroquine sensitive.

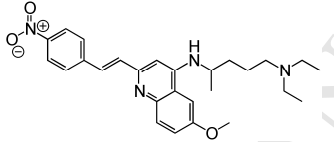
ID	Name	Structure	EC ₅₀ Dd2 (μM)	EC ₅₀ 3D7 (μM)	EC ₅₀ HepG2 (μM)
UCF 501	4-NITRO STYRYLQUINOLINE (NSQ)		0.067± 0.008	0.119 ± 0.003	12.92 ± 0.07

Table 2. Physicochemical properties of UCF 501

clogP is the calculated log octanol/water partition coefficient; Fsp3 is the fraction of *sp*³ hybridized carbon atoms.

Property	UCF 501
Molecular Weight (g/mol)	462.6
clogP	3.76
Fsp3	0.37
Number of H Bond Donor	1
Number of N Atoms	4
Polar Surface Area (Å ²)	83.2
Aqueous Solubility pH 7.4 (µg/mL)	289.7
Permeability pH 7.4 (-logPe)	2.9
Mouse Microsome Stability (% remaining at 60 min)	47.8
Microsomal stability t _{1/2} (min)	56.2
Guidelines: Aqueous solubility: <10 µg/ml-low; 10-60 µg/ml-moderate; >60-high Reference Permeability (-logPe) at pH 7.4: Verapamil-HCl 2.7; metoprolol- 3.6; rantidine- >5.9. Verapamil-HCl is considered highly permeable, metoprolol is moderately permeable; and rantidine is poorly permeable.	

Table 3. Structure activity relationship of SQ analogues

EC₅₀ values (±SD) are derived from 3 independent experiments, each with 3 replicates.

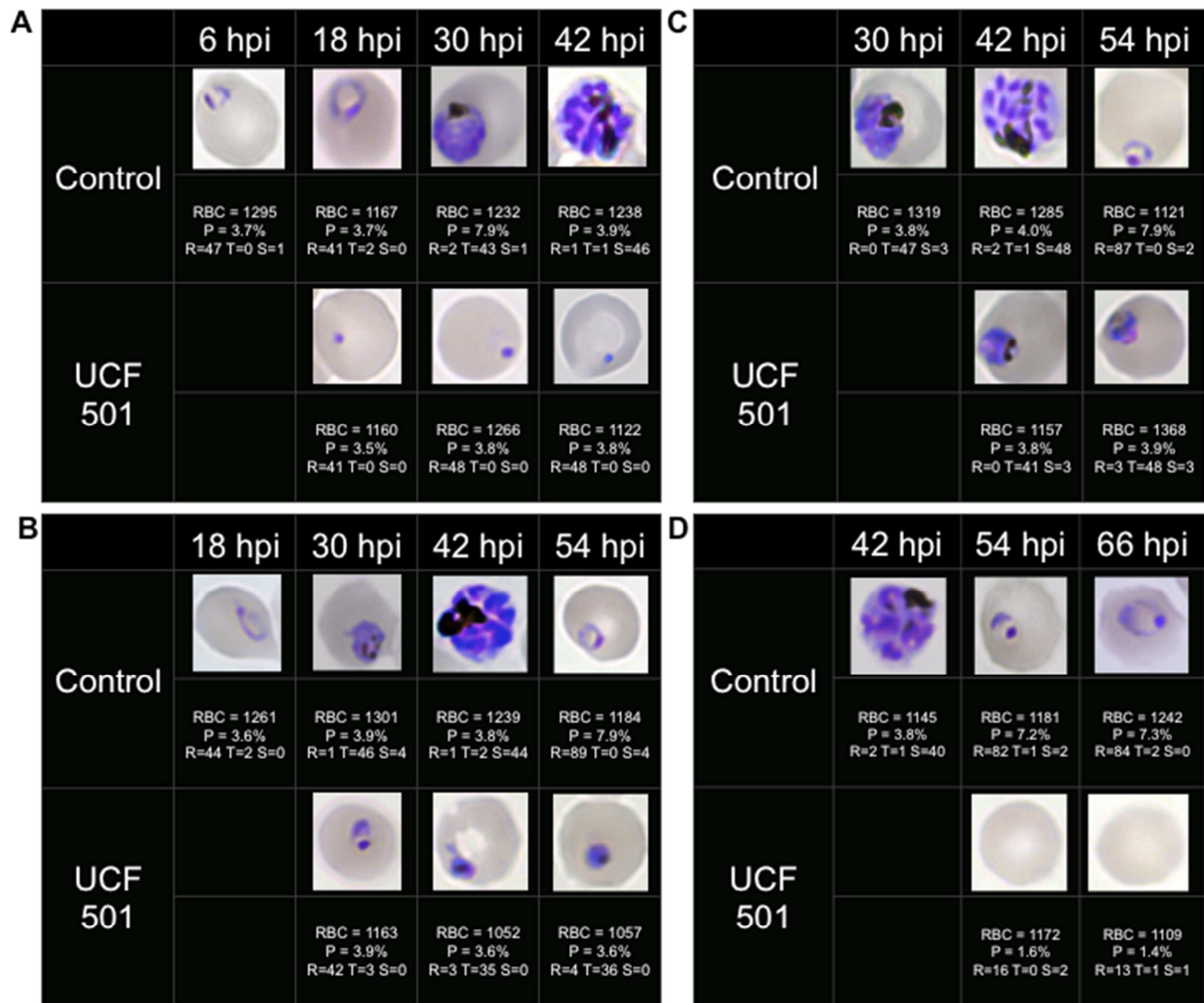
Entry	SQ	Dd2 EC ₅₀ (μM)	3D7 EC ₅₀ (μM)	HepG2 EC ₅₀ (μM)
1	8	0.323 ± 0.04	0.302 ± 0.01	19.9 ± 0.04
2	9	0.137 ± 0.05	0.299 ± 0.04	12.6 ± 0.01
3	10	0.726 ± 0.04	0.605 ± 0.04	>20
4	11	0.138 ± 0.06	0.294 ± 0.06	14.9 ± 0.03
5	12	0.057 ± 0.03	0.197 ± 0.02	15.3 ± 0.05
6	13	0.303 ± 0.04	0.373 ± 0.03	18.0 ± 0.04
7	14	0.208 ± 0.04	0.310 ± 0.02	13.6 ± 0.05
8	15	0.735 ± 0.06	0.599 ± 0.03	>20
9	16	0.471 ± 0.08	0.322 ± 0.04	12.8 ± 0.02
10	17	0.123 ± 0.05	0.193 ± 0.05	15.7 ± 0.07
Chloroquine		0.172 ± 0.02	0.011 ± 0.002	>20

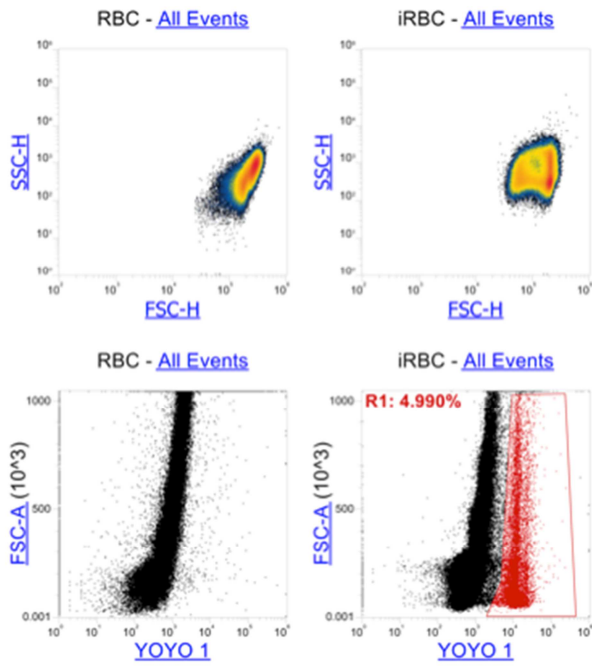
Table 4. UCF 501 does not inhibit β -hematin formation

Chloroquine, a known inhibitor of β -hematin formation, along with 8-Hydroxyquinoline, a non-inhibitor, and UCF 501 were tested at a concentration of 100 μ M for β -hematin formation inhibition using the NP-40 assay. These results are the average of two separate experiments. Compounds were tested at 100 μ M.

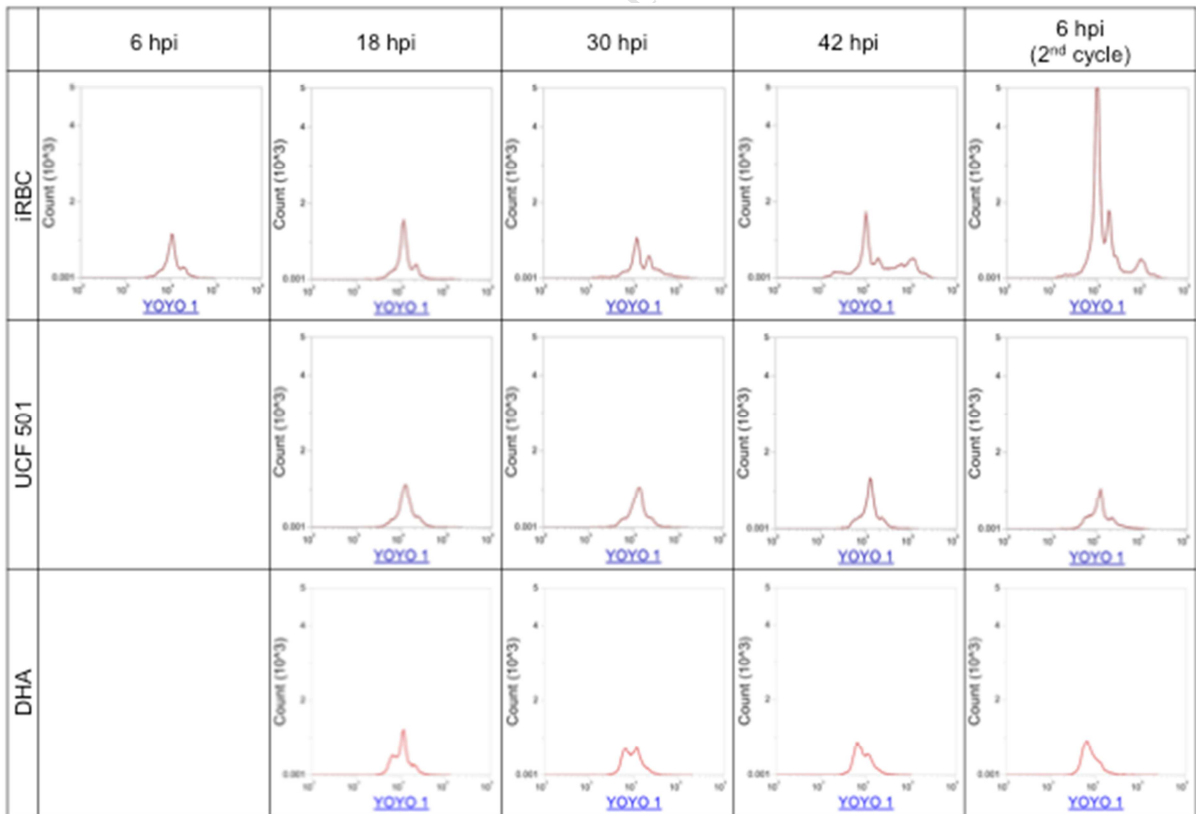
Drug/Compound	%Inhibition
Chloroquine	100 \pm 1.78
8-Hydroxyquinoline	6 \pm 0.42
UCF 501	0 \pm 0.07

3 Fig 2.

4
5

6 **Fig 3.**7 **A**

8

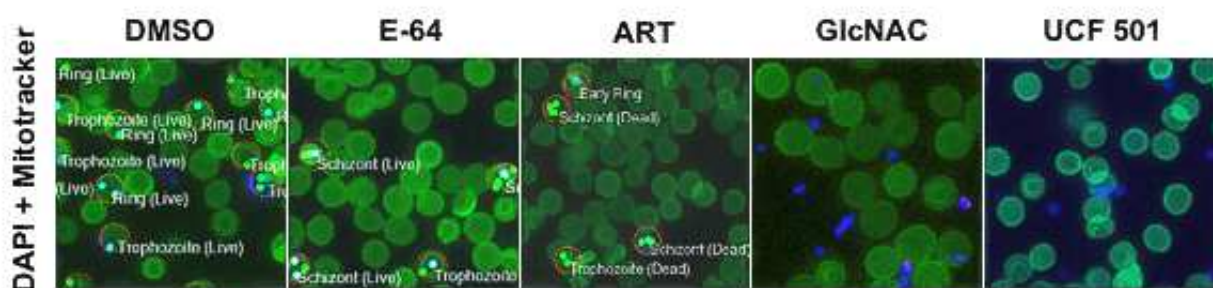
9 **B**

10

11

12 **Fig 4.**

13



14

15

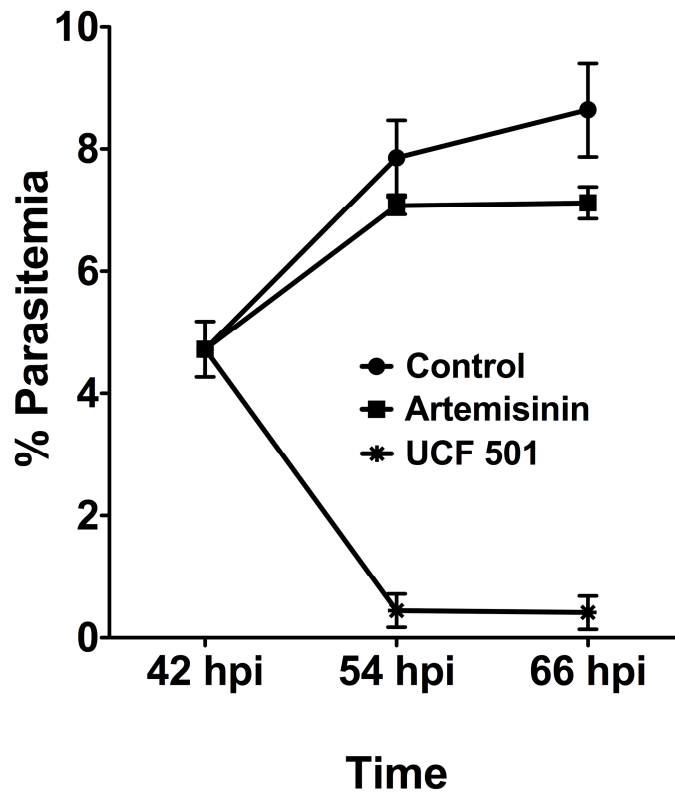
16

ACCEPTED MANUSCRIPT

17 **Fig 5.**

18

19

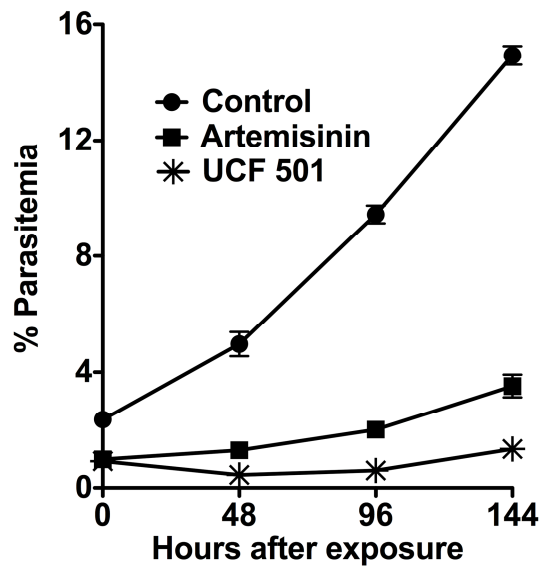


20

21

22 Fig 6.

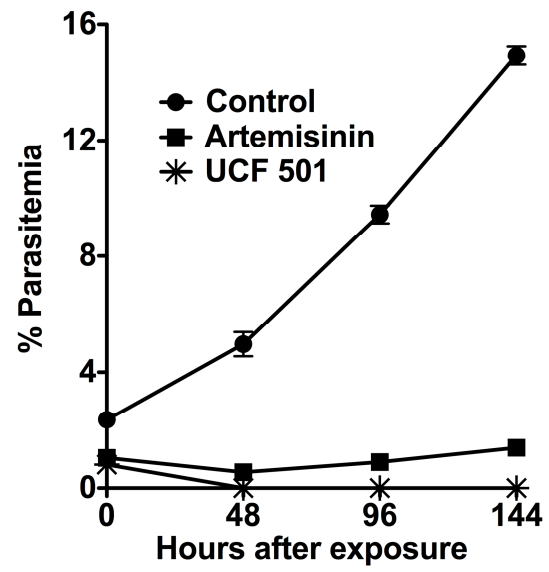
23 A



24

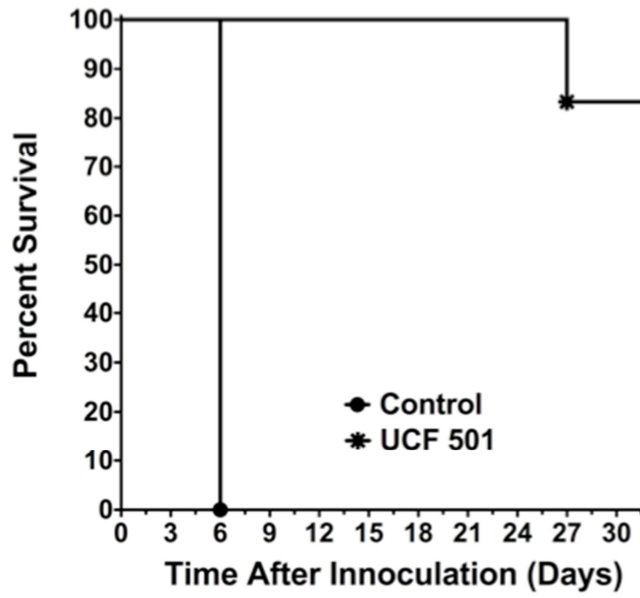
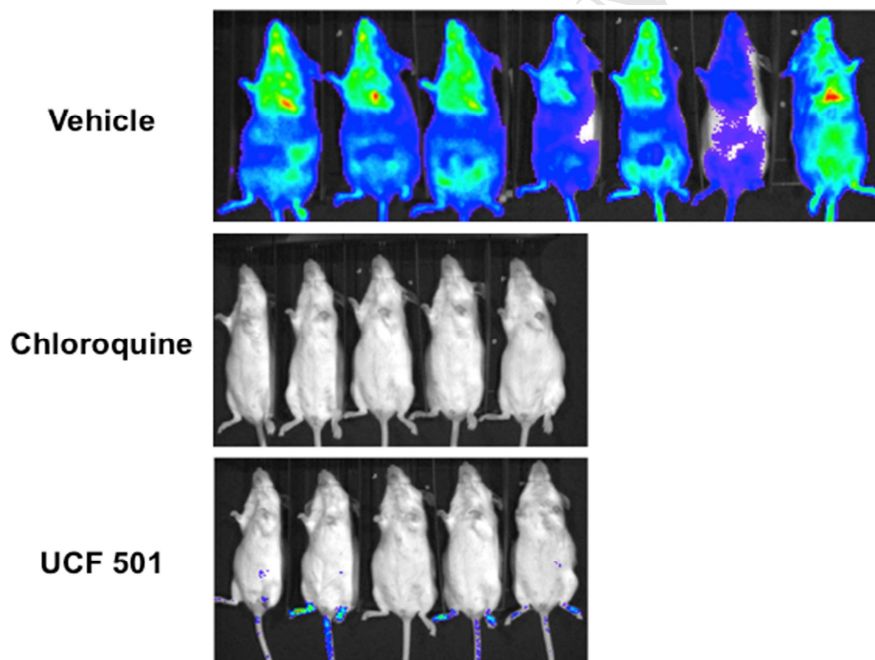
25

B



26 **Fig 7.**

27

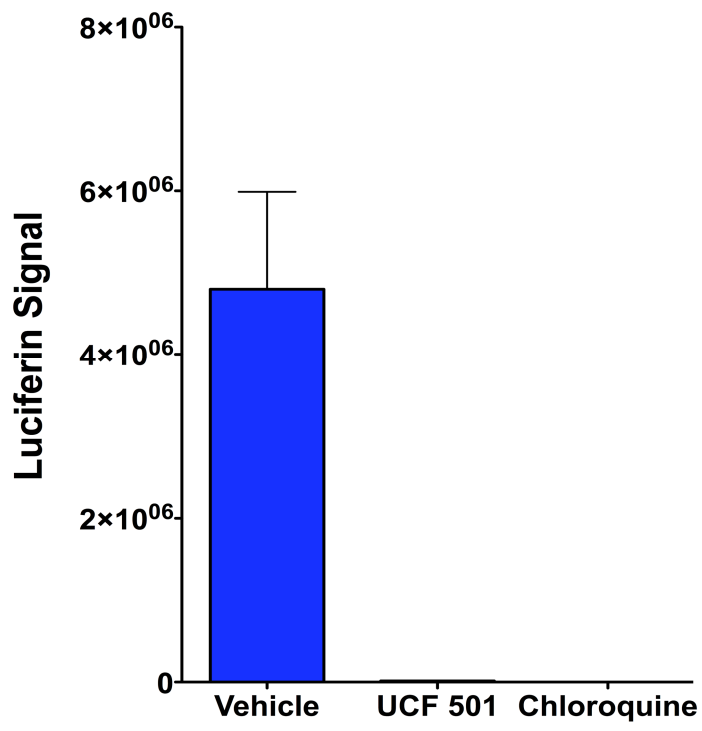
28 **A**29
3031 **B**

32

33

34

35

36 **C**

37